

## Coexisting stable patterns in a reaction-diffusion system with reversible Gray-Scott dynamics

Hitoshi Mahara,<sup>1,2</sup> Kosuke Suzuki,<sup>1,3</sup> Rumana Akther Jahan,<sup>1,3</sup> and Tomohiko Yamaguchi<sup>1</sup>

<sup>1</sup>*Nanotechnology Research Institute, National Institute of Advanced Industrial Science and Technology (AIST), AIST Central 5-2, 1-1-1 Higashi, Tsukuba 305-8565, Japan*

<sup>2</sup>*CREST, Japan Science and Technology Agency (JST), 4-1-8 Motomachi, Kawaguchi 332-0012, Japan*

<sup>3</sup>*Graduate School of Pure and Applied Sciences, University of Tsukuba, 1-1-1 Tennoudai, Tsukuba, Ibaraki 305-8571, Japan*

(Received 19 November 2007; revised manuscript received 7 September 2008; published 16 December 2008)

It is unlikely that a dissipative reaction-diffusion system exhibits static domains composed of different pattern elements. So far as we know, there is only one exception in the energy conserving system: the generalized Swift-Hohenberg (GSH) system [M.F. Hilali *et al.*, Phys. Rev. E **51**, 2049 (1995)]. Our paper reports that both a spot-domain and a line-domain coexist in a dissipative reaction-diffusion system with the reversible Gray-Scott dynamics. The system has the features that a local perturbation induces the self-rearrangement of the pattern elements and/or self-replication of spots. These features and controllability of the pattern are different from those in the GSH system.

DOI: [10.1103/PhysRevE.78.066210](https://doi.org/10.1103/PhysRevE.78.066210)

PACS number(s): 89.75.Kd, 82.40.Ck, 05.65.+b, 82.20.Wt

Pattern formations have been studied for many years as typical phenomena in dissipative systems. Among many types of patterns, typical ones are spatiotemporal patterns such as spirals [1] and target patterns [2], and static Turing patterns [3–7]. Turing patterns also have a rich variety typified by spots and lines in a two-dimensional (2D) system [3–5], and lamellae and gyroid structure in a three-dimensional (3D) system [6,7].

Concerning a system that is governed by the free energy function, on the other hand, it is filled with one kind of pattern elements such as a spot or a line. This nature seems to be an attribute of the system that asymptotically reaches to thermodynamic equilibrium; Nonomura and Ohta showed mathematically and numerically that the final state of an A-B block copolymer system is filled with one of two pattern elements even if both exist at the beginning [3]. So far as we know, there is only one exception which is known as a generalized Swift-Hohenberg (GSH) system, where the final static pattern may be covered by the two stable pattern elements (i.e., two types of domains) [4].

Similarly, most dissipative reaction-diffusion systems are filled with only one kind of pattern element. In fact, Ermentrout proved mathematically that a reaction-diffusion system cannot show bistability (spots and lines) when the system size is as small as one wavelength of the Turing pattern [8]. Even if a system is large enough and initially has two kinds of pattern elements, one of them shall be dominant at the end and the other appears just as defects [5]. Therefore it has been thought unlikely that a reaction-diffusion system supports more than two domains composed of different pattern elements at the same time. In nature, however, we can observe a variety of coexisting patterns on the skin of fish and animals. Such patterns can be reproduced numerically in an appropriate reaction-diffusion system if spatial inhomogeneity is introduced through the bifurcation parameter [9]. Thus coexisting patterns were demonstrated experimentally as well as numerically in a system with a ramp [10,11].

The main goal of this paper is to show that spots and lines can coexist in a dissipative reaction-diffusion system. This work stands on the reversible Gray-Scott (rGS) model [12,13], which is a variant of the Gray-Scott (GS) model by

Pearson [5]. The difference is the existence of the backward reactions, which is introduced in order to calculate the entropy production in pattern formation processes [12]. Similar to the GS model, the rGS model shows various patterns when the rate constants of the backward reactions are sufficiently small [13]. On the other hand, any patterns finally become static for any value of parameters when the rate constants of the backward reactions are large enough [13]. Therefore various static patterns can be examined in terms of the entropy production by using the rGS model.

As discussed below, implementation of a coexisting pattern in this system is associated with the autonomous control of the distance among the pattern elements (i.e., wave number) against local perturbations. The behavior and stability of the coexisting pattern is brought about by the interaction between the pattern elements. So far, the interaction between spots has been studied in many reaction-diffusion systems [10–12], and the mathematic basis of their repulsive nature is revealed [11]. To the authors knowledge, however, the interaction between a spot and a line, and between lines as well, has not been reported yet. Thus we investigate to clarify the importance of their repulsive nature for the self-rearrangement of pattern elements and the stability of the coexisting pattern.

The reversible Gray-Scott (rGS) model consists of three variables:  $U$ ,  $V$ , and  $P$ . The set of the reaction-diffusion equations of this model is

$$\frac{\partial U}{\partial t} = -UV^2 + f(1-U) + k_r V^3 + D_U \nabla^2 U,$$

$$\frac{\partial V}{\partial t} = UV^2 - (f+k)V - k_r V^3 + k_r P + D_V \nabla^2 V,$$

$$\frac{\partial P}{\partial t} = kV - k_r P - fP + D_P \nabla^2 P, \quad (1)$$

where  $f$  is the flow rate;  $k$  and  $k_r$  are the forward and the backward reaction rate constants, respectively. Here we assume the same rate constant  $k_r$  for all backward reactions.

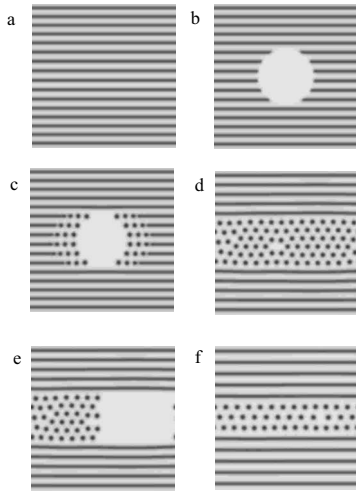


FIG. 1. A pattern formation when  $f=0.04$ ,  $k=0.082$ . The gray scale exhibits the concentration of  $U$  [0.0 (black) to 1.0 (white)]. (a) The pattern before the system is perturbed. (b) The initial pattern ( $t=0.0$ ). A circular region is perturbed to be the stable point ( $U, V, P$ )=(1.0, 0.0, 0.0). The diameter of the circle is 200 in  $dr$  unit. (c) The pattern in progress ( $t=1500.0$ ). The disconnected line turns into spots. (d) The final pattern ( $t=580\,000.0$ ). (e) The initial pattern in another simulation ( $t=0.0$ ). The right half region of the spot domain is perturbed into the stable point. (f) The final pattern developed from (e) ( $t=1\,850\,000.0$ ).

The diffusion coefficients of  $U$ ,  $V$ , and  $P$  are given as  $D_U$ ,  $D_V$ , and  $D_P$ , respectively, and are set to be  $D_U=2.0 \times 10^{-5}$ ,  $D_V=1.0 \times 10^{-5}$ , and  $D_P=1.0 \times 10^{-6}$ .

This rGS model distributed in a 2D reaction-diffusion system is calculated under periodic boundary conditions. The horizontal and the vertical direction are represented by  $x$  and  $y$ , respectively. The resolution of time is  $dt=0.25$ , and that of space is  $dr$  ( $=dx=dy$ )=0.005. The system size is  $512 \times 512$  in  $dr$  unit. The finite difference method is applied to the diffusion terms, and integration is conducted by the third Runge-Kutta method.

A typical pattern that has two pattern elements is shown in Fig. 1(d). This pattern appears through the following process. First, a stable stripe pattern composed of 16 straight lines is prepared [Fig. 1(a)]. None of these lines have open ends (tips) because of periodic boundary conditions. At the beginning, a circular subarea of the system is perturbed [Fig. 1(b)] by changing the values of  $U$ ,  $V$ , and  $P$  to those of a stable steady state of the reaction (1.0, 0.0, and 0.0, respectively). The six lines are cut by this perturbation to get open ends. Then, deformation of pattern occurs spontaneously. The perturbed lines are gradually fragmented into spots from the open ends [Fig. 1(c)]. As a result, all of the lines with open ends turn into spots. In spite of vacant space existing nearby, these spots do not self-replicate but rearrange their locations by themselves in an almost hexagonal alignment with some defects. In the course of this rearrangement, the average distance between spots reaches 35.73 (in  $dr$  unit hereafter) [Fig. 1(d)], whereas the distance between nonperturbed lines increases from 32 to 33.67 (measured at  $x=256$ ). The average distance between the line and the spots slightly increases to be 32.75. In this way, the distances between the pattern ele-

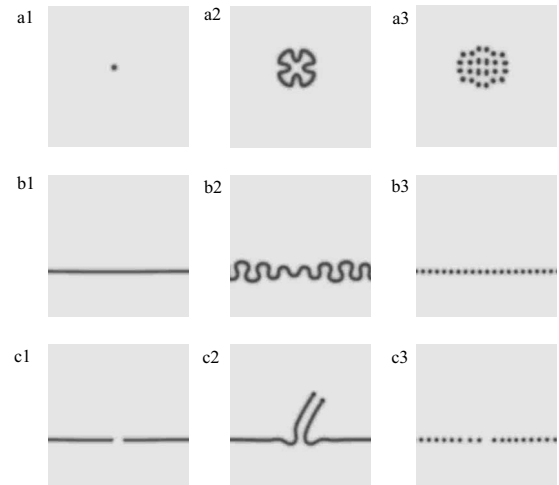


FIG. 2. (a1)–(a3) Examples of the pattern development from a single spot. (a1) An example of the initial pattern ( $k=0.082$ ,  $t=0.0$ ). (a2) The pattern in progress. The pattern extends to the vacant region radially ( $k=0.077$ ,  $t=10\,000.0$ ). (a3) Another example of pattern in progress. The spots self-replicate repeatedly ( $k=0.08$ ,  $t=21\,000.0$ ). (b1)–(b3) Examples of the pattern development from a single line without tips (a loop line). (b1) An example of the initial pattern ( $k=0.082$ ,  $t=0.0$ ). (b2) The pattern in progress. The line becomes winding ( $k=0.078$ ,  $t=20\,000.0$ ). (b3) Another example of pattern in progress. The line is broken into spots ( $k=0.083$ ,  $t=20\,000.0$ ). (c1)–(c3) Examples of the pattern development from a single line with tips. (c1) An example of the initial pattern ( $k=0.082$ ,  $t=0.0$ ). (c2) The pattern in progress. The line starts to extend ( $k=0.0795$ ,  $t=16\,000.0$ ). (c3) Another example of pattern in progress. The line is broken into spots ( $k=0.084$ ,  $t=1000.0$ ).

ments increase spontaneously after perturbation.

Further perturbation gives a hint for the mechanism of the rearrangement process [Figs. 1(d)–1(f)]. At the beginning, a half of the domain filled with spots in Fig. 1(d) is perturbed as before. Then the number of spots is reduced to 44 from 81 [Fig. 1(e)]. Again, rearrangement of pattern occurs spontaneously; the spots do not self-replicate nor disappear, but rearrange their hexagonal alignment by themselves. Concomitantly, the lines move apart from each other, and finally the pattern becomes stable [Fig. 1(f)]. The three average distances between the spots, the lines, and the spot and the line are 40.41, 40.0, and 39.19, respectively, again in  $dr$  unit. Thus the average distances between the pattern elements become larger than those in the initial pattern in Fig. 1(d).

For the coexisting pattern to be implemented, both lines and spots must be realized stably under the same parameter conditions. In order to know how the stabilities and the behaviors of spots and lines depend on the parameter  $k$ , we carry out numerical calculations to observe the time evolution of pattern elements in the following three cases: a single spot, a line without tips (a loop), and a finite line with tips [Fig. 2; (a1), (b1), and (c1), respectively]. A single spot is stable if  $0.081 < k \leq 0.0915$ , and a loop is stable if  $0.0795 < k \leq 0.0825$ . Notice that there exists a bistable region ( $0.081 < k \leq 0.0825$ ) where both a single spot and a loop are stable. On the other hand, a finite line is unstable in this bistable region, and the line turns into the stable spots [(c3)

in Fig. 2]. This explains why the spots appear sandwiched by the lines [Fig. 1(d)]; the loop is stable but becomes no more stable once it gets open ends by perturbation, and the consequent finite line turns into alternatively stable spots through the sequential fragmentation.

When the parameter  $k$  is small, the isolated pattern element may grow. Some examples of pattern-growing processes are summarized in Fig. 2. For example, a single spot expands radially to become a loop [(a2) in Fig. 2,  $0.077 < k \leq 0.0785$ ]. If  $k$  is much larger, a spot grows to be a line by extending its tips (not shown,  $0.0785 < k \leq 0.0795$ ). Therefore the coexisting pattern cannot be realized by the perturbation applied in Fig. 1 because the spots change themselves into lines in these parameter regions. Further increase of  $k$  ( $0.0795 < k \leq 0.081$ ) results in the continuous self-replication of spots [(a3) in Fig. 2].

A loop grows to meander at  $0.077 < k \leq 0.0795$  [(2b) in Fig. 2], and the tips of a line extend at  $0.077 < k \leq 0.081$  [(c2) in Fig. 2]. These behaviors mean that the pattern elements have a tendency to fill the vacant space. These patterns grow dense until the mutual distance between the neighboring pattern elements becomes sufficiently small. Thus, even though the coexisting pattern is realized, the distances between the pattern elements cannot be widened by such perturbation as in Fig. 1 in these parameter regions.

The behaviors of these patterns are simple when the parameter  $k$  is large. A single spot disappears if  $k$  is larger than 0.0915. Even a loop is fragmented to become spots ( $0.0825 < k \leq 0.084$ ) or disappears ( $0.084 < k$ ). Therefore, no line can be stable, and consequently, the coexisting pattern cannot be realized when  $k > 0.0825$ .

The above-mentioned parameter scans indicate that there is a bistable region where both a spot and a line can be stable. Then, we may expect the possibility for implementation of the coexisting pattern in this bistable region. Figure 3 shows the parameter region where a single spot is stable (between the bold lines: region S) and the region where a single line is stable (between the dotted lines: region L). Outside right of the right dotted line, a line becomes spots [as in Fig. 2(b3)] or disappears. Thus we cannot expect any coexisting patterns, as the line is not stable. Indeed, we examined but could not observe any coexisting patterns in this parameter region.

On the other hand, both pattern elements are stable where the regions S and L are superimposed (region  $\alpha$ ). It is the region where the coexisting pattern can be observed. However, in order to realize such coexisting patterns as in Figs. 1(d) and 1(f), appropriate initial pattern should be given for each set of parameters. For example, for the set of parameters  $f=0.04$  and  $k=0.0825$ , the number of the lines in the initial line pattern [something like Fig. 1(a)] should be reduced to be 12 [Fig. 4(b)]. Otherwise, for example, the initial pattern with 16 lines turns into all spots [Fig. 4(a)]. This result strongly suggests the importance of the density of pattern elements for their stability and the coexisting pattern.

In the left side of the region S in Fig. 3, a spot becomes either a line or self-replicated. If a spot can only self-replicate, the coexisting pattern can be realized because the morphology of the pattern element is preserved even after the self-replication of spots is completed. Indeed, in the pa-

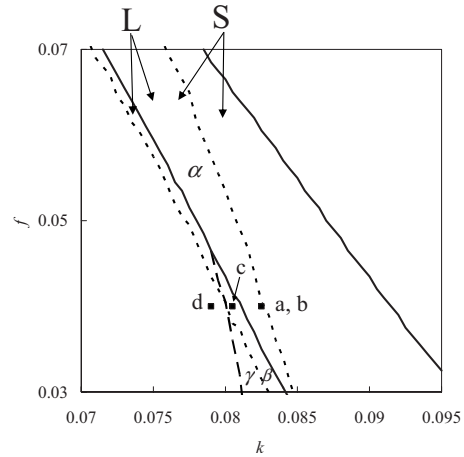


FIG. 3. The phase diagram. A single spot is stable in the region S that is enclosed by the bold line. A single line is stable in the region L that is enclosed by the dotted line. In the superimposed region of these two regions (region  $\alpha$ ), the coexisting pattern is realized. The coexisting pattern is realized also in the region  $\beta$  that is enclosed by three lines: the bold line, the dashed line, and the dotted line. In the region  $\gamma$  that is enclosed by the dashed line and the dotted line, the coexisting pattern is realized, too. The points  $a-d$  show the parameter conditions for the calculations shown in Fig. 4.

parameter regions  $\beta$  and  $\gamma$  in Fig. 3, the spot can only self-replicate and finally the coexisting pattern can be observed. A typical example is given in Fig. 4(c). The initial pattern for this calculation is the same as that in Fig. 1(f). Some of the spots self-replicate and the number of the spots increases to be 74. Then the spots rearrange themselves into an almost hexagonal array, and the pattern becomes static. As a result, the distance between the pattern elements becomes shorter than that of the initial pattern. That is, in the final pattern, the average distance between spots is 35.89; between lines: 34.89; and between spots and lines: 33.36 in  $dr$  unit. Therefore, in this parameter region, we can say that the coexisting pattern does not increase the distance between the pattern elements against the pattern-erasing perturbation.

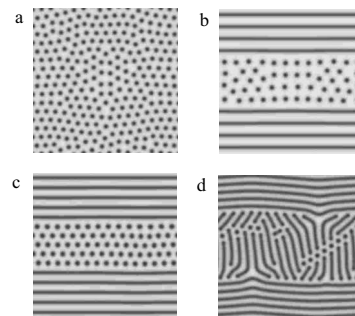


FIG. 4. (a) and (b) A pattern formation when  $f=0.04$ ,  $k=0.0825$ . (a) The pattern when the initial pattern has 16 straight lines ( $t=10\,000.0$ ). (b) The pattern when the initial pattern has 12 straight lines ( $t=130\,000.0$ ). For the perturbation, see Fig. 1(b). (c) A stable pattern at  $f=0.04$ ,  $k=0.0805$ ,  $t=11\,000.0$ ; (d) A stable pattern at  $f=0.04$ ,  $k=0.079$ ,  $t=30\,000.0$ . The initial patterns in both cases are the same as in Fig. 1(d).

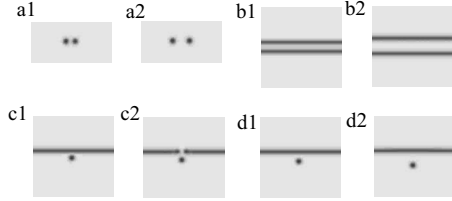


FIG. 5. (a1) and (a2) The behavior of the system that has only two spots ( $f=0.04$ ,  $k=0.082$ ). The size of the system ( $x \times y$ ) is  $256 \times 128$  in  $dr$  unit. (a1) The initial pattern ( $t=0.0$ ). The distance between the spots is 30. (a2) The pattern when  $t=100\,000.0$ . The distance increases to 52. (b1) and (b2) The behavior of the system that has only two straight lines without tips ( $f=0.04$ ,  $k=0.082$ ). The size of the system ( $x \times y$ ) is  $256 \times 256$ . (b1) The initial pattern. The distance between the lines is 29. (b2) The pattern when  $t=100\,000.0$ . The distance increases to 48. (c1) and (c2) The behavior of the system that has one spot and one straight line without tips ( $k=0.082$ ). (c1) The initial pattern. The distance between the spot and the line is 22. (c2) The pattern in progress ( $t=500.0$ ). The line is cut. (d1) and (d2) The behavior of the system that has one spot and one straight line without tips ( $k=0.082$ ). (d1) The initial pattern. The distance between the spot and the line is 30. (d2) The pattern in progress. The spot moves apart from the line. The distance is 47 when  $t=50\,000.0$ .

Contrarily, the coexisting pattern cannot be realized in the left side of the regions  $\alpha$ ,  $\beta$ , and  $\gamma$ . Figure 4(d) shows an example of the pattern formation in this region. In this calculation, the initial pattern has the same configuration as that of Fig. 1(f). Some spots and the lines with tips are going to be mixed in the domain of the spots, where the lines are slightly bending. Finally, the pattern becomes static with no spot domains.

As mentioned above, it seems that the interaction between the pattern elements determines whether the coexisting pattern can be realized or not. We therefore investigate the local interaction between the pattern elements in the following three cases for  $f=0.04$ : (i) a spot and another spot, (ii) a line and another line, and (iii) a spot and a line.

(i) The system that has only two spots is calculated in the parameter region where the single spot is stable. An example is shown in Fig. 5(a) ( $f=0.04$ ,  $k=0.082$ ). At the beginning, the distance between the spots is 30 in  $dr$  unit [Fig. 5(a1)]. The spots start to move apart from each other, and the distance becomes 52 at  $t=1.0 \times 10^5$  [Fig. 5(a2)]. Thus there is a repulsive force between spots in this parameter region.

(ii) All the same as in the previous case, the loop lines get away from each other. An example is shown in Fig. 5(b) ( $f=0.04$ ,  $k=0.082$ ); the distance between lines is initially 29 [Fig. 5(b1)], and becomes 48 at  $t=1.0 \times 10^5$  [Fig. 5(b2)]. This increase in the distance is observed in the parameter region where the line without tips is stable ( $f=0.04$ ,  $0.0795 < k \leq 0.0825$ ).

(iii) Now we examine the interaction between the spot and the line in the bistable parameter region ( $f=0.04$ ,  $0.081 < k \leq 0.0825$ ) where both the spot and the loop line are stable. In this case, the change in the loop line depends on the distance from the spot. The loop line is cut when the initial distance is sufficiently small. An example is shown in the sequence in Fig. 5(c). Initially, the

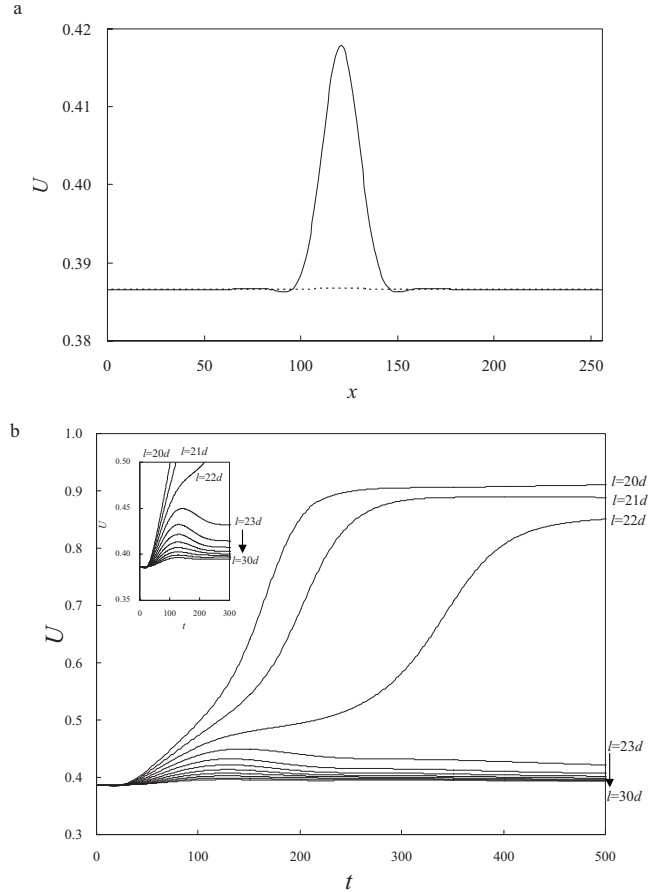


FIG. 6. (a) The horizontal profiles of  $U$  along the bottom of the line. The solid line shows the profile of the line when a spot exists near the line. The initial distance between the spot and the line is 23 (in  $dr$  unit). The profile at  $t=100.0$  is plotted. The dashed line shows the profile of the line when the system has only one straight line. (b) The maximum  $U$ 's of the line on the vertical direction ( $x=122$ ) are plotted as a function of time. These values represent the peaks like in Fig. 4(a). The behavior of the line depends on the initial distance between the spot and the line. If the distance is smaller than 22, the peak increases monotonically. If the distance is larger than 23, the peak increase at first and then it goes back to the initial state.

distance is set 22 [Fig. 5(c1)]. After a while, the loop line is cut and the tips appear [Fig. 5(c2)]. As the finite line is unstable in this parameter region, it will turn into spots. Contrary, the loop line is not cut but coexists with the spot when the initial distance is sufficiently large [Fig. 3(d)]. At the beginning, the distance between the spot and the loop line is set at 30 [Fig. 5(d1)]. Then the line remains stable, and the spot moves apart from the line. At  $t=5.0 \times 10^4$ , the distance reaches 47 [Fig. 5(d2)]. These results in Figs. 5(c) and 5(d) suggest that the spot affects the line.

The influence of the spot to the line can be discussed through the profile of the line. Figure 6(a) plots the minimum values of  $U(x)$  along the line ( $f=0.04$ ,  $k=0.082$ ). The profile is almost flat when the system has only one straight line. On the other hand, the profile has a peak at the nearest distance to the spot when the system has both a line and a spot. The time series of this peak are plotted in Fig. 6(b). The line is



not cut if the initial distance is larger than 23 in  $dr$  unit. In this case, the peak height increases at the beginning. After a while the peak begins to decrease monotonically and converges to the initial state by increasing the distance. This behavior means that the line recovers its stability by changing the distance from the spot. In contrast, the line is cut when the distance is smaller than 22. The peak height increases monotonically even though the distance increases with time. Therefore, in this case, the critical initial distance whether the line will be cut or not should be between 22 and 23.

The results in Fig. 6 suggest that the profile of the line reaches is identical to that of the isolated stable line when the distance between the line and the spot is large enough. Moreover, the maximum value of these time series becomes lower as the initial distance increases. It means that the influence of the spot on the line becomes smaller as the distance increases. Thus we can deduce that two pattern elements (spots and lines) can coexist when the distances among the pattern elements are sufficiently large. In other words, there exists the critical distance between the pattern elements, above which they can exist stably.

In all three cases, the pattern elements exhibit a repulsive nature similar to that in other models [14–16]. This nature causes the rearrangement of the pattern as shown in Fig. 1. This repulsive nature brings about the coexisting pattern even though the line tends to wind itself. Such an example is found in the parameter region  $\gamma$  in Fig. 3. As the self-replication process of spots is faster than the winding process of the line, the spots quickly fill the vacant region. As a result, the spots push the lines to suppress the winding nature of the line. However, the distances between the pattern elements will not become shorter than the critical value for the line to be cut. Therefore the line domains are preserved and coexist stably with the spot domains.

It is noteworthy that the coexisting pattern is realized in the bistable region  $\alpha$  and the region ( $\beta$  and  $\gamma$ ) in Fig. 3, and that the characteristics of the coexisting pattern in these parameter regions are different from each other. In the regions  $\beta$  and  $\gamma$ , the spots self-replicate if there remains vacant spaces or the distance between the pattern elements is sufficiently large. In this case the pattern becomes static after the pattern elements are adequately packed. Therefore the pat-

tern has both the upper and the lower limits of the distances. This feature looks like that of the Turing instability [18] even though the mechanisms of both pattern formations are quite different. In the Turing instability, the effect of the diffusion drives the system from a stable fixed point to an unstable saddle point. This instability induces Turing patterns that emerge from the initially homogeneous state (which corresponds to a stable fixed point) by adding small white noise with respect to space. Thus the wavelength in the Turing instability is restricted to the bounded value that is determined by the reaction rates and the diffusion coefficients in the system. In the present case, on the other hand, patterns cannot emerge from such initial conditions but from the initial distribution of pattern elements or spatially inhomogeneous perturbation [13]. This difference (or limitation) in the present model is originated from the self-replicating and repulsive nature of pattern elements.

Contrarily, in the bistable region  $\alpha$ , the pattern elements cannot grow. Thus the pattern elements may only leave each other to preserve their morphologies if there is a vacant space. Therefore there is no upper limit of the distance between the pattern elements. This feature reminds us of the Alder transition [17] in which the repulsive force among the elements keep themselves apart from each other to result in an equally spaced packing. The repulsive nature is different from that of the Turing instability. This feature enables us to control the number of spots and the distance between the pattern elements; the number can be reduced and the distance is increased with perturbations in the bistable region. In the GSH system also, lines and spots coexist; however, the pattern is pinned, and reconfiguration of the pattern does not occur. Therefore such controllability of spots is the characteristic attribute of the present system and cannot be expected in the GSH system. We thus summarize that the coexisting pattern in the present rGS system is realized by the nature of the self-arrangement of the pattern elements or by the self-replication of the spots, or both.

We thank Dr. Shoji and Dr. Ohta for fruitful discussions. This work was conducted under the research program “Creation of Novel Nano-material/system Synthesized by Self-Organization for Medical Use,” Core Research for Evolutional Science and Technology (CREST), Japan Science and Technology Agency (JST).

- 
- [1] R. Kapral and K. Showalter, *Chemical Waves and Patterns* (Kluwer, Dordrecht, 1995).
- [2] H. Nagashima, *J. Phys. Soc. Jpn.* **60**, 393 (1989).
- [3] M. Nonomura and T. Ohta, *J. Phys.: Condens. Matter* **13**, 9089 (2001).
- [4] M'F. Hilali, S. Metens, P. Borckmans, and G. Dewel, *Phys. Rev. E* **51**, 2046 (1995).
- [5] J. E. Pearson, *Science* **261**, 189 (1993).
- [6] H. Shoji, K. Yamada, and T. Ohta, *Phys. Rev. E* **72**, 065202(R) (2005).
- [7] A. V. Korylyuk and J. G. E. M. (Hans) Fraaije, *J. Chem. Phys.* **125**, 164716 (2006).
- [8] B. Ermentrout, *Proc. R. Soc. London, Ser. A* **434**, 413 (1991).
- [9] K. M. Page, P. K. Maini, and N. A. M. Monk, *Physica D* **202**, 95 (2005).
- [10] P. Borckmans, A. De Wit, and G. Dewel, *Physica A* **188**, 137 (1992).
- [11] E. Dulos, P. Davis, R. Rudovics, and P. De Kepper, *Physica D* **98**, 53 (1996).
- [12] H. Mahara, N. J. Suematsu, T. Yamaguchi, K. Ohgane, Y. Nishiura, and M. Shimomura, *J. Chem. Phys.* **121**, 8968 (2004).

- [13] H. Mahara, T. Yamaguchi, and M. Shimomura, *Chaos* **15**, 047508 (2005).
- [14] K. Krischer and A. Mikhailov, *Phys. Rev. Lett.* **73**, 3165 (1994).
- [15] S.-I. Ei and J. Wei, *Jpn. J. Ind. Appl. Math.* **19**, 181 (2002).
- [16] Y. Nishiura, T. Teramoto, and K.-I. Ueda, *Phys. Rev. E* **67**, 056210 (2003); *Chaos* **15**, 047509 (2005).
- [17] B. J. Alder and T. E. Wainwright, *J. Chem. Phys.* **33**, 1439 (1960); *Phys. Rev.* **127**, 359 (1962).
- [18] A. M. Turing, *Philos. Trans. R. Soc. London, Ser. B* **237**, 37 (1952).